

Analysis of the Sn chain length fluctuations on Si(100)2 × 1: An extraction of microscopic parameters

M. Kučera,* P. Kocán, P. Sobotík, K. Majer, and I. Ošťádal

Faculty of Mathematics and Physics, Charles University, Prague, Czech Republic

(Received 6 March 2017; revised manuscript received 21 June 2017; published 24 July 2017)

Tin chains grown on the Si(100)2 × 1 surface were studied by scanning tunneling microscopy. Real time measurements were used for recording chain length fluctuations in a temperature range from 310 to 350 K. The recorded data were analyzed by means of a statistical model containing both interfering processes observed at a chain termination—random attachment and detachment of metal atoms. Rates of the both processes were calculated from lifetimes of two different chain terminations (monomer or dimer) by means of derived formulas. The activation energies for the detachment and frequency prefactors were calculated from dependence of the corresponding time constants on temperature in an Arrhenius plot. A similar approach was used for characterization of binding Sn atoms on *C*-type defects which represent preferential adsorption sites.

DOI: [10.1103/PhysRevB.96.045430](https://doi.org/10.1103/PhysRevB.96.045430)

I. INTRODUCTION

Submonolayer metal nanostructures grown on oriented silicon surfaces attract an interest due to a large variety of potential applications based on developed silicon technology. The experimental techniques of scanning tunneling microscopy (STM) and atomic force microscopy (AFM) provided unique, atomically resolved data on surface morphology, electronic structure, and surface processes. Obtained experimental data considerably contributed to the latest progress in understanding growth processes and are of great importance for further development of techniques and for comparison with theoretical calculations. But some parameters of processes controlling the growth at the atomic level remain unknown. Especially an experimental determination is valuable—either for comparison with theoretical results or for kinetic modeling of the growing system under certain conditions.

The Si(100)2 × 1 surface is composed of dimers arranged into rows and it represents a natural template for spontaneous growth of ordered linear structures. Submonolayer deposition of group-III or group-IV metals on Si(100)2 × 1 results in formation of well-defined one-dimensional (1D) chains of metal atoms [1–4]. The metal chains grow perpendicularly to the dimer rows and also consist of dimers which are aligned parallel to silicon dimers and positioned above the trenches between the silicon dimer rows. This work deals with Sn chains grown on the Si(100)2 × 1 surface. According to *ab initio* calculations [5] the most stable configuration of a tin dimer is a buckled one (the dimer is not parallel to the surface). However at room temperature the dimers within the chains look symmetric on STM images and are buckled only at certain conditions [6].

The growth of the chains is generally accepted to follow the surface polymerization reaction proposed by Brocks and Kelly [1], in which chain ends act as nucleation centers for diffusing atoms. Some surface defects can also act as the nucleation centers. Three basic types of defects are usually observed on the Si(100)2 × 1 surface—one missing silicon dimer (*A*-type defect), more than one neighboring missing silicon dimers

(*B*-type defect) and a dissociated molecule of water (*C*-type defect) [7–10]. From all the defects only the *C*-type defects were reported as nucleation centers for In [11] and Ga [12] and similar behavior is expected in the cases of Al and Pb [13].

Additionally to standard STM imaging, other alternative STM techniques were used throughout the time to acquire genuine experimental data—an *in vivo* technique [14] for surface imaging during the deposition of In [15,16] and a line scanning method for recording spontaneous detachment of atoms terminating grown In chains [17] at room temperature (RT). In published literature growth models based on the experimental data were used for kinetic Monte Carlo (kMC) simulations of submonolayer growth of Ga [18], In [16], and Al [19], determination of diffusion barriers [16,19,20], and investigation of the role of *C* defects at metal adatom adsorption [21]. The observed detachments of metal adatoms complicates the study of growth by means of kMC simulations. Additional unknown parameters—activation energies for the detachment—have to be included into a model. For this reason, an effort to obtain the parameters independently is highly rational.

Activation energies of adatom detachment from the chain were previously investigated experimentally [16,17] and by means of density functional theory (DFT) for Pb [13] and group-III metals [19]. A metal chain can be terminated either by a dimer or by a single metal atom (monomer). The activation energy may depend on the origin of the detaching atom—either the dimer is decomposed (“even” atom) or the monomer escapes (“odd” atom). Neither experimental nor theoretical data have been reported yet on the stability of tin chains.

In this paper we used data from STM real time measurements at various temperatures for the calculation of parameters of spontaneous thermally activated detachment of tin adatoms terminating the chains or those trapped by *C*-type defects. We developed a model which takes into account both random processes present at a quasiequilibrium state after the deposition—adatom attachment and detachment. The model was used for the analysis of time series representing the occurrence of studied events. Finally we obtained activation energies and frequency prefactors for Sn adatom detachment from the chains with both types of the termination and from the *C*-type defects.

*Corresponding author: mikucer@gmail.com

II. EXPERIMENT

Experiments were performed in an ultrahigh vacuum chamber with a base pressure $< 3 \times 10^{-9}$ Pa equipped with a noncommercial STM head of our design. We used Sb-doped samples with a resistivity of $0.014 \Omega \text{ cm}$. The tin was evaporated from a tantalum crucible in a resistively heated tungsten gasket approximately 30 min after preparation of the silicon surface reconstruction. All samples were prepared at room temperature with an average coverage of 0.04 ML (1 ML = $6.78 \times 10^{14} \text{ cm}^{-2}$), if not otherwise stated. The deposition rate was 0.0003 ML/s. Samples were heated by a direct passing current and the sample temperature was determined from the supplied power and a calibration curve. The temperature calibration for a steady state was performed at the same conditions and sample configuration by means of a subtle thermocouple glued to the silicon substrate of a standard size used at experiments. The uncertainty of the determined temperature was ± 5 K.

A tip position at STM measurements was at the center of the sample (between the electrodes). Half of the DC heating voltage was used for a correction of the set tunnel voltage.

Detachment and attachment processes were recorded by means of a line scanning method. It is based on repetitive scanning of a single line chosen from the investigated area. A direction of scanned lines is aligned with the chains and a standard STM image is recorded until the STM tip reaches the chosen chain. At this moment the tip motion in the direction perpendicular to the lines is stopped and scanning continues repeatedly only over the chosen chain (until it is interrupted). This procedure considerably enhances the rate of recording the chain length evolution. Events of tin adatom detachment and attachment can be monitored with a time resolution of approximately 0.1 s.

III. RESULTS AND DISCUSSION

A. Stability of tin chains

Growth of metal chains on anisotropic Si(100) 2×1 surface is kinetically determined. Possible detachment of terminating atoms from the chains plays an important role in a growth scenario [16,21,22]. The exchange rate of atoms among growing chains during the deposition determines how far the grown structure is from the equilibrium. The adatom exchange continues after the deposition and even after film relaxation. The exchange constitutes a dynamic equilibrium state and the rate of events depends on temperature. Due to the adatom detachment and attachment the length of particular chains may change with time (fluctuate) but the growth characteristic—chain length distribution—remains unchanged in a steady state. We assume that we performed our measurements at such a situation.

The process of atom exchange among the chains is visible on sequence of STM empty state images in Figs. 1(a)–1(f). One end of the chosen chain (marked by a white arrow) is anchored on a C-type defect, where the chain nucleation started. Figure 1 shows gradual detachments of individual atoms from the free end of the chain. Imaging started at a chain length of nine atoms [see Fig. 1(a)] and ended up at the length of four atoms [see Fig. 1(f)]. During the detachment

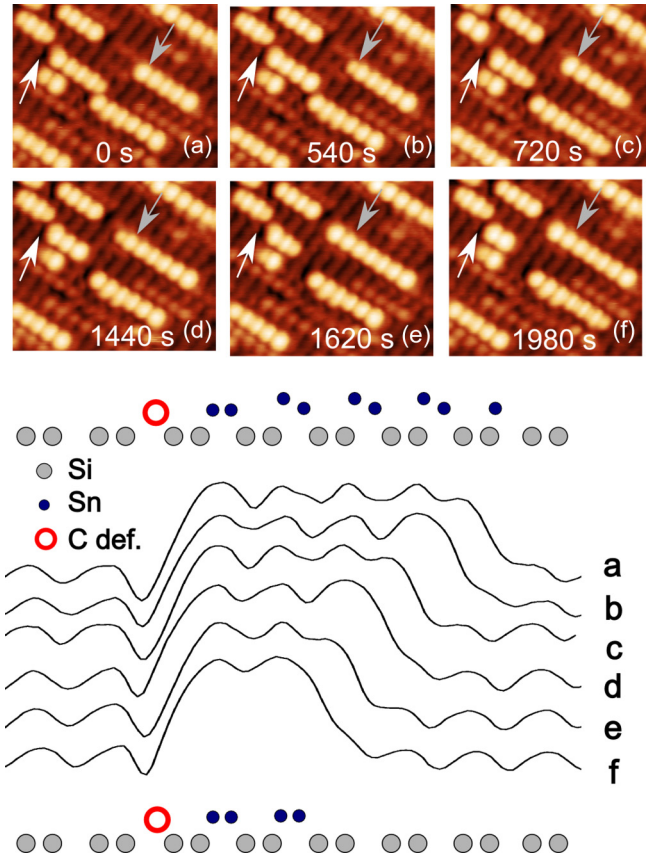


FIG. 1. (a)–(f) Shortening of the tin chain nucleated at a C-type defect (empty state images— $U_s = -2$ V, $I = 0.3$ nA—of area $7.5 \text{ nm} \times 7.5 \text{ nm}$ taken at room temperature with coverage 0.1 ML). The six representative images were picked from a larger record of a fluctuating chain in order to demonstrate monotonically decreasing chain length. Line profiles of the chains marked by the white arrows are shown below the set of images. Buckling of dimers in the chain when terminated by a single atom can be recognized. Additional faint traces of the chains visible on the images are caused by doubling the very tip.

the chain is alternately terminated by monomers (odd) and dimers (even). A bright protrusion corresponding to the odd termination is in the empty state images easily distinguishable from the even termination by its smaller size and lower brightness. Corresponding profiles are on the bottom part of Fig. 1. Maxima in the profiles corresponding to the odd terminations are less pronounced than maxima in case of the even terminations. Two schematic side views of the tin atom arrangement are added for the chain with odd termination [see Fig. 1(a)] and with even termination [see Fig. 1(f)]. The STM images demonstrate atom attachments to a neighboring chain as well (marked by a gray arrow).

An interesting feature accompanying the odd termination is buckling of the dimers in the chain. The unbuckled dimers appear in the images as regular oval protrusions which can be distinguished from distorted protrusions in the case of the buckled dimers. The buckling of the dimers within the chains at room temperature was observed and reported by Glueckstein *et al.* [6] and they attributed it to the presence of another tin chain in close vicinity. Additionally to such a

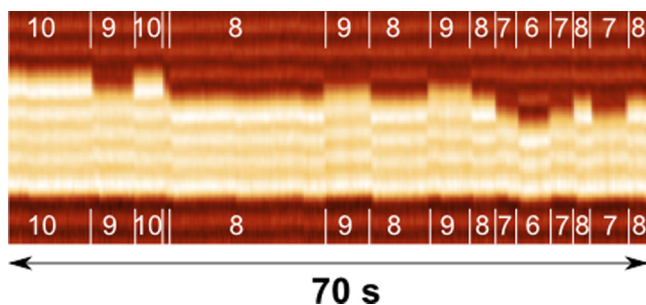


FIG. 2. An example of a line scanning measurement ($U_s = -2$ V, $I = 0.3$ nA) of a Sn chain at 326 K. The white ticks are added to guide the eye and help to recognize the segments sections of different lengths. Where it was possible the lengths of the chain were added in the lower section of the image. The lower end of the chain is anchored by a C-type defect.

behavior we observed the dimer buckling in the chains well separated from others but terminated by a monomer. The odd termination probably freezes the thermal “flip-flop motion” of dimers and the buckling appears. The STM imaging of Sn chains composed of dimers only and the thermal motion of the dimers has been already studied by *ab initio* (DFT) calculations [23], but a possible influence of a monomer termination has not been theoretically investigated. The observed sensitivity of dimer buckling on chain termination allows registering an event of detachment/attachment without imaging the chain termination and improves time resolution.

Figure 2 shows a result of one line scanning measurement. A sequence of 512 line scans records history of atom detachment/attachment at the free end of a chain during 70 s. The record is divided into segments, each of which contains the line scans at the unchanged chain length. The width of each particular line scan segment (bordered by the inserted white ticks in the image) represents the lifetime of the corresponding chain termination. The change of the length by 1 atom can be reliably distinguished and a transition between the buckled and unbuckled dimer imaging can be noticed by comparison of neighboring segments.

The chain length evolution can be described as a sequence of events—detachments and attachments—which result in transitions between the odd and even chain terminations. We consider the atom detachment from a chain as a thermally activated process and thus we distinguish two different activation energies according to the odd or even chain termination— E_a^O or E_a^E respectively. We neglect the dependence of the energy on a chain length. If the detachment is the only present process, an average time between detachment events—a time constant τ_{det} (detachment rate is $1/\tau_{\text{det}}$)—can be expressed by a formula:

$$\tau_{\text{det}}^{O,E} = \frac{1}{\nu_0^{O,E}} \exp\left(\frac{E_a^{O,E}}{kT}\right), \quad (1)$$

where k is the Boltzmann constant, ν_0 is the frequency prefactor, E_a is activation energy for detachment, and T is temperature. The indexes O or E correspond to a detachment from the odd or even termination respectively.

A statistical analysis of the experimentally obtained data in the case when the attachment process practically does not occur (at very low density of chains on the surface [16,17])

is not complicated and obtaining the mean lifetimes of chain terminations would be straightforward. In our experiments, however, there are always several chains in the close vicinity of an investigated chain and we have to take into account the attachment process. The data in Fig. 2 show frequent attachment events. The attaching atoms are atoms detached from the neighboring chains.

Even though the line-scanning technique is much faster (approximately 500 \times) than STM image recording, it is still relatively slow and possible leakage of events should be taken into account especially at room and higher temperatures. The problem in the case of the investigated processes and measurements will be discussed in a separate section together with consequences for accuracy of obtained results (see Sec. III C).

The detachments from chains with odd or even terminations represent two independent Poisson processes with average rates of $1/\tau_{\text{det}}^O$ and $1/\tau_{\text{det}}^E$ respectively. Although the rate of attachment depends on a number of atoms detached in the neighborhood of the investigated termination and local character of the potential-energy surface in the proximity of the termination (i.e., on local conditions), we consider the attachment to odd or even terminations as two other independent Poisson processes. We introduce the mean rates of attachment $1/\tau_{\text{att}}^O$ and $1/\tau_{\text{att}}^E$ representing the quantities averaged over the chain population. To determine the activation energies and corresponding frequency prefactors in the formula (1) we need to find a relation between the desired time constants and the experimentally obtained lifetimes influenced by the process of atom attachment. Because the oncoming calculations can be performed independently for even and odd terminations, we will drop the upper indexes O and E . A probability $P_0(t)$ that the termination of the chain will not change (via detachment or attachment) in a time interval $(0, t)$ is given by a formula:

$$P_0(t) = \exp\left[-t\left(\frac{1}{\tau_{\text{att}}} + \frac{1}{\tau_{\text{det}}}\right)\right]. \quad (2)$$

First we have to find simultaneous probabilities corresponding to the measured sequences of events when processes of detachment and attachment occur independently. A simultaneous probability $\Delta P(t)_{\text{det}}$ that the chain termination does not change in the time interval $(0, t)$ and only the detachment occurs in a time interval $(t, t + \Delta t)$ writes

$$\Delta P_{\text{det}}(t) = P_0(t) \left(1 - \frac{\Delta t}{\tau_{\text{att}}}\right) \frac{\Delta t}{\tau_{\text{det}}}. \quad (3)$$

The corresponding probability density function is then

$$p_{\text{det}}(t) = \lim_{\Delta t \rightarrow 0} \frac{\Delta P(t)}{\Delta t} = P_0(t) \frac{1}{\tau_{\text{det}}}. \quad (4)$$

Similarly, the probability density function for the attachment is

$$p_{\text{att}}(t) = P_0(t) \frac{1}{\tau_{\text{att}}}. \quad (5)$$

Using the probability density functions we can determine mean lifetimes of chains before the detachment $\langle t_{\text{det}} \rangle$ and before the attachment $\langle t_{\text{att}} \rangle$:

$$\langle t_{\text{det}} \rangle = \int_0^\infty t p_{\text{det}}(t) dt = \frac{\tau_{\text{det}} \tau_{\text{att}}^2}{(\tau_{\text{att}} + \tau_{\text{det}})^2} \quad (6)$$

TABLE I. The values of mean lifetimes obtained from measurements at various temperatures and corresponding calculated time constants.

Odd termination				
T (K)	τ_{det} (s)	$\langle t_{\text{det}} \rangle$ (s)	τ_{att} (s)	$\langle t_{\text{att}} \rangle$ (s)
313	14.90	7.13	33.47	3.18
317	8.09	3.58	16.06	1.80
326	5.03	2.62	13.04	1.01
332	2.48	1.63	10.53	0.38
337	1.49	0.67	3.03	0.33
342	0.53	0.37	2.69	0.07
349	0.24	0.19	1.96	0.02
Even termination				
T (K)	τ_{det} (s)	$\langle t_{\text{det}} \rangle$ (s)	τ_{att} (s)	$\langle t_{\text{att}} \rangle$ (s)
326	12.54	4.05	16.49	3.08
332	9.11	2.35	9.39	2.28
337	4.35	1.09	4.37	1.09
342	2.89	0.83	3.35	0.72
349	2.34	0.60	2.39	0.59

and

$$\langle t_{\text{att}} \rangle = \int_0^{\infty} t p_{\text{att}}(t) dt = \frac{\tau_{\text{att}} \tau_{\text{det}}^2}{(\tau_{\text{att}} + \tau_{\text{det}})^2}. \quad (7)$$

Thus the time constants corresponding to the adatom detachment/attachment from/to a chain termination are

$$\tau_{\text{det}} = \frac{(\langle t_{\text{att}} \rangle + \langle t_{\text{det}} \rangle)^2}{\langle t_{\text{det}} \rangle}, \quad \tau_{\text{att}} = \frac{(\langle t_{\text{det}} \rangle + \langle t_{\text{att}} \rangle)^2}{\langle t_{\text{att}} \rangle}, \quad (8)$$

where the values of $\langle t_{\text{det}} \rangle$ and $\langle t_{\text{att}} \rangle$ can be obtained easily from experimental data. In a case when no attachment is present, i.e., $\tau_{\text{att}} \rightarrow \infty$, then simply $\tau_{\text{det}} = \langle t_{\text{det}} \rangle$. We distinguish between detachment/attachment from/to even or odd terminations—the quantities τ_{det}^O , τ_{det}^E , and τ_{att}^O , τ_{att}^E result from the corresponding formulas.

The chain length fluctuations were measured at seven different temperatures. In order to estimate an influence of tunneling conditions we performed measurements for two different values of tunneling current and three different values of sample voltage—all at three chosen temperatures. Line scanning data obtained for various chains on the surface at the same temperature were converted into time series of attachment and detachment events and accumulated into corresponding det/att data sets which contained about 200 events for each type of chain terminations—odd or even. Corresponding time intervals were processed and the mean lifetimes of chain terminations before a detachment and before an attachment were calculated. Finally, using the formula (8), the desired time constants τ_{det} were determined for the detachments from the odd and even chain terminations at a given temperature. Table I shows the differences between the experimentally obtained mean lifetimes and corresponding time constants calculated by means of the model for the temperatures set at the measurements. The differences represent significant corrections in a case when the adatom attachment cannot be neglected.

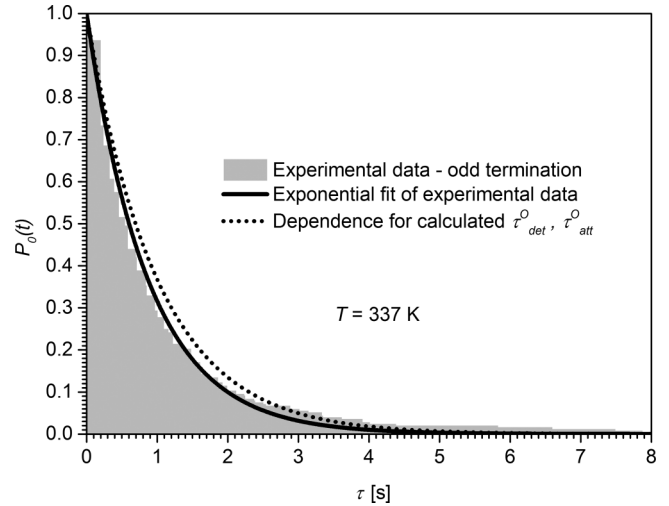


FIG. 3. A probability $P_0(t)$ that the termination of the chain will not change (via detachment or attachment) in a time interval $(0; t)$ obtained from experimental data for odd terminations fitted by the corresponding function (2).

A representative experimentally obtained histogram of the probability (2) for the odd termination is shown in Fig. 3. An exponential fit can be compared with the dependence corresponding to the calculated values of τ_{att} and τ_{det} .

In Fig. 4(a), the temperature dependence of time constants for detachment of odd terminations shows Arrhenian behavior in the whole measured temperature range for all used tunneling conditions. The time constants for detachment from even terminations [see Fig. 4(b)] exhibit Arrhenian behavior in the whole temperature range for a sample voltage of -2 V. But at a sample voltage of $+2$ V the detachment from even terminations follows the Arrhenian dependence above 325 K only. Below 325 K the calculated time constants are temperature independent, which indicates that the detachment is controlled by a different mechanism, not thermally activated but dependent on tunneling conditions. Modification of a barrier height by the tunnel voltage would result in the Arrhenian dependence, so it can be excluded. Instead, we prefer a role of electrons tunneling into empty surface states and energy released at following electron thermalization. A similar competition between thermally activated and tip induced hops between adsorption positions of indium atoms on Si(100) surface at lower temperatures was observed at experimental determination of surface adatom mobility [20].

Using the formula (1) for linear fitting the dependence of $\ln(\tau_{\text{det}}^{O,E})$ on reciprocal temperature provides both the activation energy and the frequency prefactor for the investigated process (see Fig. 4).

We fitted the natural logarithm of Eq. (1) in the temperature ranges, where the detachment can be considered as thermally activated, by a linear function weighted by the uncertainties of the measured time constants. The activation energies and frequency prefactors obtained from the fits are $E_a^O = 0.88 \pm 0.08$ eV, $\nu_0^O = 10^{13 \pm 1}$ s $^{-1}$; $E_a^E = 1.02 \pm 0.08$ eV, $\nu_0^E = 10^{14 \pm 1}$ s $^{-1}$. The resulting activation energies show that an even atom at the end of the Sn chain is bound

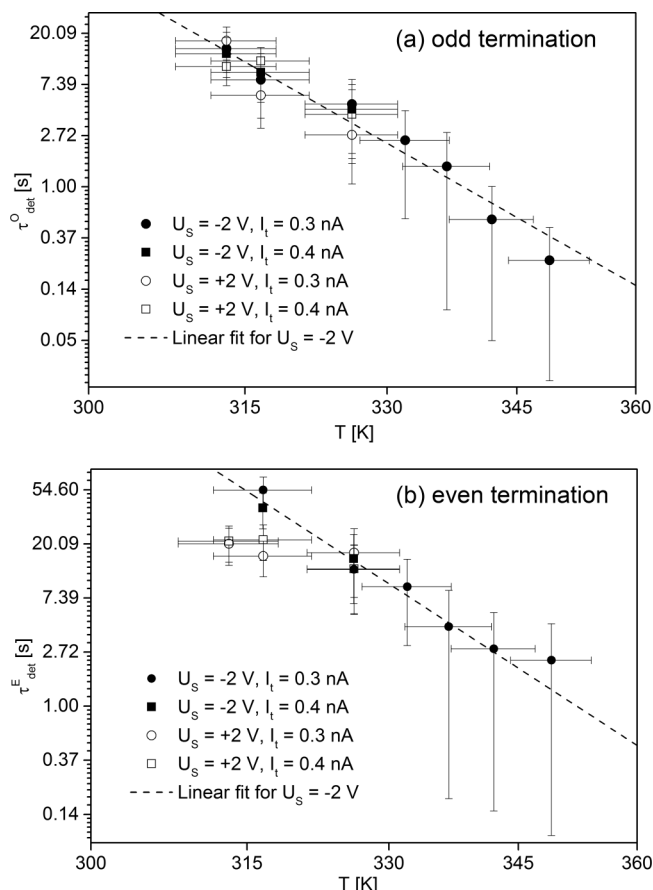


FIG. 4. Temperature dependence of time constants for (a) odd and (b) even terminations of tin chains on various scanning conditions. The temperature axis is in a reciprocal scale.

more strongly than the odd one—the difference in activation energies for detachment is 0.14 eV.

The only reported data (DFT calculations), which can be compared with our results, concern the other group-IV metal—Pb [13]. Authors showed that the adsorption energy of a Pb chain terminated by the dimer is higher in comparison with the single atom termination—the difference is less than 0.1 eV and practically does not depend on a chain length.

B. Interaction with *C*-type defects

A similar approach was used for investigation of average time before detachment of tin adatoms trapped on *C*-type defects. Figure 5 shows a sequence of STM images of the same area on the sample taken at 350 K. The white arrow indicates a position of the *C*-type defect with a tin chain anchored to it. In this sequence atoms attach to and detach from the free end of the chain until there remains only the *C*-type defect. Then a diffusing atom is trapped by the defect and evolution of a new chain begins again.

From the recorded events we extracted time intervals between the trapping of an adatom by a *C*-type defect and either attachment of another adatom or detachment of the trapped adatom. The analysis of the time intervals provided mean lifetimes $\langle t_{\text{det}} \rangle$, $\langle t_{\text{att}} \rangle$ and finally using the formula (8) we obtained time constants τ_{det} .

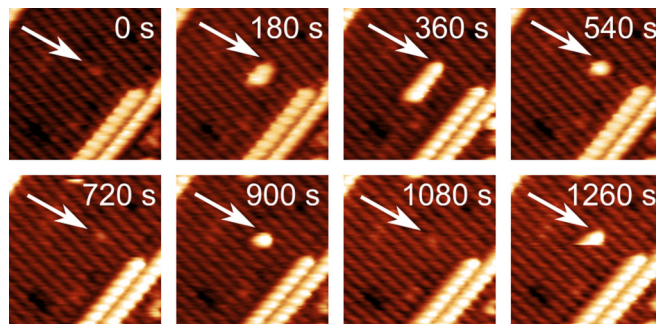


FIG. 5. Sequence of STM images taken at 350 K. $U_s = -2$ V, $I = 0.3$ nA. An arrow marks the position of a *C*-type defect.

For STM measurements we used the tunneling conditions, for which we expected no influence of the tip on the observed processes ($U_s = -2$ V and $I = 0.3$ nA). The dependence of $\ln(\tau_{\text{det}})$ on reciprocal temperature is shown in Fig. 6.

The activation energy for detachment of a single Sn atom from a *C*-type defect and frequency prefactor obtained from the linear fit are $E_a^{C\text{def}} = (0.86 \pm 0.08)$ eV, $\nu_0^{C\text{def}} = 1 \times 10^{12 \pm 1}$ s $^{-1}$. The values do not differ much from the values characterizing the detachment of adatoms from the odd terminations. The activation energy can be compared with the only reported value—0.8 eV—calculated for detachment of a Pb atom from *C*-type defect by Pieczyrak and Jurchyszyn [13].

C. Unrecorded events and accuracy of calculated activation energies

Accuracy of the obtained results is determined statistically by experimental data assuming that data contain whole information on investigated processes. The used line scanning measurement provides data obtained by “sampling” the chain length with limited time resolution. Here we estimate probability of lost (unrecorded) events and consequences for the accuracy of results.

We have to distinguish two possible scenarios resulting in a “zero event” which appears when two reverse events appear consecutively (attachment + detachment or vice versa) between the sampling moments:

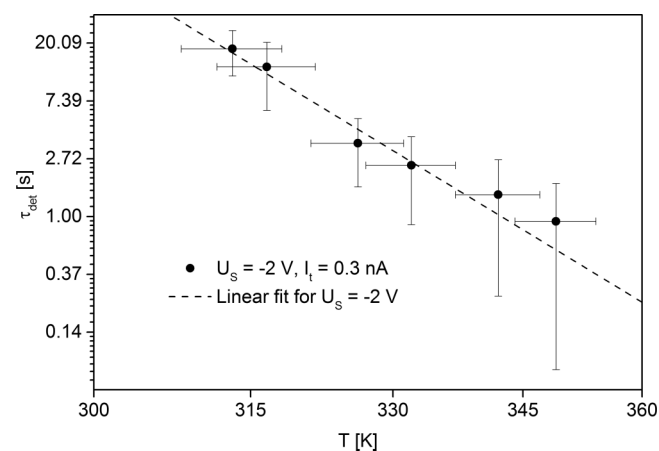


FIG. 6. Temperature dependence of the time constants for adatom detachment from a *C*-type defect. The temperature axis is in a reciprocal scale.

(i) A detached atom returns back after a random walk. The thermally activated surface mobility of the Sn atom is high enough to suppose a possible return into an initial position within a sampling period (0.14 s). At room and higher temperatures a return probability depends in practice on concentration of capture positions in neighborhood (captured atom fails to return back). Due to this scenario we miss a certain number of detachment events. We can estimate a corresponding correction by means of a simple Monte Carlo simulation of random walk on a square lattice. The simulation provides statistics of a number of atoms returning back versus a number of atoms finding another capture position. The concentration of the capture positions is generated to correspond with observed morphologies. As a result we found out that at given chain concentration (0.1%) about 70% of detachment processes fall into “zero events” by fast reattachment of the detached atom. We note that the percentage does not strongly depend on the concentration of the chains. Due to extremely fast migration of atoms on the bare surface, the percentage of missed detachment events is practically temperature independent. Consequently all obtained time constants are approximately three times lower and the value of corrected prefactor should be approximately $3\times$ higher, while the values of the activation energies are not affected.

(ii) The “zero event” is composed of detachment and attachment of two different atoms, which is a slower mechanism. The values of calculated time constants of the Poisson processes are much higher than a time scale of used sampling so an existence of missing events on the set time scale can be excluded.

Finally it can be seen that uncertainty of results calculated from the experimental data fully covers correction estimated for unrecorded “zero events.”

IV. CONCLUSION

STM observations of Sn structures showed that at RT most of the tin chains nucleate on *C*-type defects. Two different

terminations of the grown chains were observed—dimer or single atom (referred to as even or odd respectively). Real time STM observations (line scanning method) were used for recording chain length fluctuations. We demonstrated that the odd termination induces the dimer buckling in the chain (additionally to the buckling induced by another neighboring chain reported in literature before).

We developed a statistical model for data analysis which allowed calculation of activation energies and frequency prefactors for detachment of Sn atoms from both types of chain terminations. The values after the correction for unrecorded events are

$$E_a^O = (0.88 \pm 0.08) \text{ eV}, \quad \nu_0^O = 3 \times 10^{13 \pm 1} \text{ s}^{-1}$$

and

$$E_a^E = (1.02 \pm 0.08) \text{ eV}, \quad \nu_0^E = 3 \times 10^{14 \pm 1} \text{ s}^{-1}.$$

The only exception from the Arrhenius behavior was found for data obtained at a sample voltage of +2 V and temperatures <325 K when the tip induced detachments dominate.

Finally the line scanning method was used to determine the activation energy and frequency prefactor for detachment of a single Sn atom from the *C*-type defect. The corrected result is

$$E_a^{C\text{def}} = (0.86 \pm 0.08) \text{ eV}, \quad \nu_0^{C\text{def}} = 3 \times 10^{12 \pm 1} \text{ s}^{-1}.$$

The results show that the adatom attachment rate, which depends on local conditions around a particular chain termination, can be assumed in the model as a parameter averaged over the whole investigated chain population. The developed model possesses a certain universality and can be used when an effect of two competing processes is studied.

-
- [1] G. Brocks, P. J. Kelly, and R. Car, *Phys. Rev. Lett.* **70**, 2786 (1993).
- [2] A. A. Baski, J. Nogami, and C. F. Quate, *J. Vac. Sci. Technol. A* **8**, 245 (1990).
- [3] A. A. Baski, J. Nogami, and C. F. Quate, *J. Vac. Sci. Technol. A* **9**, 1946 (1991).
- [4] A. A. Baski, C. F. Quate, and J. Nogami, *Phys. Rev. B* **44**, 11167 (1991).
- [5] L. Magaud, A. Pasturel, L. Jure, P. Mallet, and J. Y. Veuillen, *Surf. Sci.* **454-456**, 489 (2000).
- [6] J. C. Glueckstein, M. M. R. Evans, and J. Nogami, *Surf. Sci.* **415**, 80 (1998).
- [7] R. J. Hamers and U. K. Koehler, *J. Vac. Sci. Technol. A* **7**, 2854 (1993).
- [8] J.-H. Cho, K. S. Kim, S.-H. Lee, and M.-H. Kang, *Phys. Rev. B* **61**, 4503 (2000).
- [9] P. Sobotík and I. Ošťádal, *Surf. Sci.* **602**, 2835 (2008).
- [10] O. Warschkow, S. R. Schofield, N. A. Marks, M. W. Radny, P. V. Smith, and D. R. McKenzie, *Phys. Rev. B* **77**, 201305 (2008).
- [11] P. Kocán, L. Jurczyszyn, P. Sobotík, and I. Ošťádal, *Phys. Rev. B* **77**, 113301 (2008).
- [12] P. Kocán, P. Sobotík, and I. Ošťádal, *Phys. Rev. B* **74**, 037401 (2006).
- [13] B. Pieczyrak and L. Jurczyszyn, *Appl. Surf. Sci.* **304**, 91 (2014).
- [14] I. Ošťádal, P. Kocán, P. Sobotík, and J. Pudl, *Phys. Rev. Lett.* **95**, 146101 (2005).
- [15] I. Ošťádal, J. Javorský, P. Kocán, P. Sobotík, and M. Setvín, *J. Phys.: Conf. Ser.* **100**, 072006 (2008).
- [16] J. Javorský, M. Setvín, I. Ošťádal, P. Sobotík, and M. Kotrla, *Phys. Rev. B* **79**, 165424 (2009).
- [17] P. Kocán, P. Sobotík, I. Ošťádal, J. Javorský, and M. Setvín, *Surf. Sci.* **601**, 4506 (2007).
- [18] M. A. Albao, M. M. R. Evans, J. Nogami, D. Zorn, M. S. Gordon, and J. W. Evans, *Phys. Rev. B* **72**, 035426 (2005).

- [19] M. A. Albao, C.-H. Hsu, D. B. Putungan, and F.-C. Chuang, *Surf. Sci.* **604**, 396 (2010).
- [20] M. Setvín, J. Javorský, Z. Majzik, P. Sobotík, P. Kocán, and I. Ošťádal, *Phys. Rev. B* **85**, 081403 (2012).
- [21] P. Kocán, P. Sobotík, I. Ošťádal, M. Setvín, and S. Haviár, *Phys. Rev. E* **80**, 061603 (2009).
- [22] V. I. Tokar and H. Dreyse, *Phys. Rev. B* **74**, 115414 (2006).
- [23] T.-L. Chan, C. Z. Wang, Z.-Y. Lu, and K. M. Ho, *Phys. Rev. B* **72**, 045405 (2005).